CHIN. PHYS. LETT. Vol. 38, No. 5 (2021) 055203

Numerical and Experimental Evaluation of Shine-Through Loss and Beam Heating Due to Neutral Beam Injection on EAST

Jin-Fang Wang(王进芳)[1*], Ying-Ying Li(李颖颖)[2], Bin Wu(吴斌)[1], Yu-Qing Chen(陈玉庆)[1], Jun Li(李军)[1], Yong-Jian Xu(许永建)[1], Long-Xi Chen(陈龙溪)[3], Bao-Long Hao(郝保龙)[4], Deng Zhou(周登)[1], Juan Huang(黄娟)[1], Si-Ye Ding(丁斯晔)[1], Zhen Yang(杨振)[1], Ya-Wei Hou(侯雅巍)[5,6*], Xiao-Juan Liu(刘晓娟)[1], and Nong Xiang(项农)[1]

[1]*Institute of Plasma Physics, Chinese Academy of Sciences, Hefei 230031, China*
[2]*ENN Fusion Technology R&D Center, Langfang 065001, China*
[3]*School of Information Engineering, Shandong Youth University of Political Science, Ji'nan 250103, China*
[4]*Advanced Energy Research Center, Shenzhen University, Shenzhen 518060, China*
[5]*CAS Key Laboratory of Geospace Environment and Department of Plasma Physics and Fusion Engineering, University of Science and Technology of China, Hefei 230026, China*
[6]*KTX Laboratory and Department of Plasma Physics and Fusion Engineering, University of Science and Technology of China, Hefei 230026, China*

(Received 26 January 2021; accepted 16 March 2021; published online 2 May 2021)

This research applies experimental measurements and NUBEAM, ONETWO and TRANSP modules to investigate the shine-through (ST) loss ratio and beam heating percentage of neutral beam injection on EAST. Measurements and simulations confirm that the ST loss ratio increases linearly with beam energy, and decreases exponentially with plasma density. Moreover, using the multi-step fitting method, we present analytical quantitative expressions of ST loss ratio and beam heating percentage, which are valuable for the high parameter long-pulse experiments of EAST.

DOI: 10.1088/0256-307X/38/5/055203

Neutral beam injection is one of the major auxiliary heating methods on modern tokamaks. The ionization of injected neutral particles in a plasma will lead to a large number of fast ions. A considerable number of theoretical and experimental studies have been carried out on the confinement and loss of fast ions, as well as their effects on plasma confinement and MHD instabilities.[1−4] However, the injected neutral particles that are not ionized by the collisions with the background plasma will pass directly through the plasma and hit the inner wall opposite the injection window in tokamak. This loss of beam power is called the shine-through (ST) loss. Since EAST is a fully superconducting tokamak, the injection angle and tangential radius of neutral beam injection are limited.[5] This feature leads to the great ST loss on EAST under certain plasma conditions,[5,6] which seriously affects the safety of the fusion device. In addition, in the high parameters and long pulse operation, the serious ST loss will degrade the performance of the plasma. Therefore, it is crucial to know the ST loss to offer an accurate amount of the total power deposition and to improve the whole discharge performance.

Since the neutral beam injection (NBI) penetration depth $\lambda_{\rm NB}$ can be expressed as $\lambda_{\rm NB} \sim (E_{\rm nbi}/A_{\rm nbi})/n_{\rm e}$, the ST loss is closely related to the beam energy and the plasma density. $E_{\rm nbi}$, $A_{\rm NBI}$ and $n_{\rm e}$ are the beam energy, the mass number of the neutral beam species and the electron density of the plasma, respectively.[7] The ST loss on EAST has been investigated in different beam injection angles,[5,8] beam energy and plasma density.[6] On DIII-D, the ST loss has also been measured again using the data from the temperature rise of the thermocouples embedded in the beam target tiles of the tokamak vessel.[9] The results indicate that the ST loss ratio decreases exponentially with the plasma density and increases linearly with the beam energy. In the construction and experiment of ITER, the ST loss has also been evaluated[7,10,11] to achieve the minimum density during plasma discharges for the safety of tokamak. Therefore, an analysis of ST loss is essential for the tokamaks with NBI. However, there are only the qualitative trends of ST loss with plasma density and beam energy. Thus, the systematic quantitative evaluation of the ST loss ratio during EAST discharges is necessary, especially for the upgraded EAST NBI system. There are many neutral beam injec-

Supported by the Collaborative Innovation Program of Hefei Science Center, CAS (Grant No. 2019HSC-CIP015), the National Natural Science Foundation of China (Grant Nos. 11875290, 1170529, 11875253, and 11975276), the Fundamental Research Funds for the Central Universities (Grant No. WK3420000004), the Anhui Provincial Natural Science Foundation (Grant No. 2008085J04), and the National Key Research and Development Program of China (Grant No. 2019YFE03020004).
*Corresponding authors. Email: jfwang@ipp.ac.cn; arvayhou@ustc.edu.cn
© 2021 Chinese Physical Society and IOP Publishing Ltd

tion modules, such as NUBEAM,[12] ASTRA,[13] and NBEAMS.[14] According to the comparisons of the different codes,[12] the Monte-Carlo NUBEAM module and the transport ONETWO[15] and TRANSP[16] modules are adopted in our simulation to evaluate the ST loss ratio ($P_{\rm ST}/P_{\rm inj}\times 100\%$, where $P_{\rm ST}$ is the ST loss and $P_{\rm inj}$ is the injected beam power) and the total beam heating percentage with injected beam power and plasma density on EAST.

The initial EAST NBI system is displayed in Fig. 1(a). In this figure, the beamlines are named NBI-A at the A port and NBI-F at the F port. Each beamline consists of two beam paths. These two beamlines were initially arranged as a balanced injection (i.e., NBI-A is co-current and NBI-F is counter-current) to investigate the ITER-like low input torque. However, during the physical experiment on EAST, it was found that there was a lot of beam power loss. Among them, the prompt loss was especially high at about 50% for NBI-F.[17] Thus, to improve beam power deposition and reduce the loss, in the following upgraded NBI system the beamline at the F port will be installed at the D port with the injection direction changed from counter-current to co-current, as shown in Fig. 1(b). The detailed descriptions of the injection direction and tangential radius for different neutral beams used in this study are shown in Table 1.

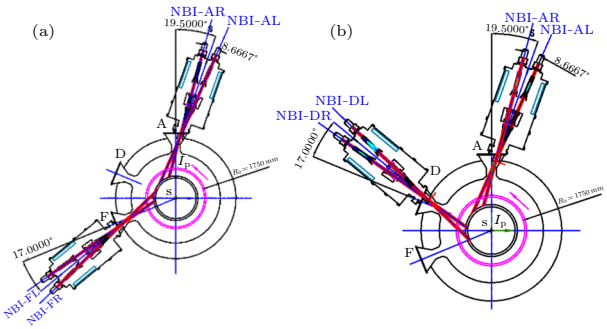

Fig. 1. Schematic of (a) initial and (b) upgraded EAST NBI systems.

Table 1. Neutral beams with the different injection directions and tangential radius $R_{\rm tan}$ on EAST.

Beams	NBI-AL	NBI-AR	NBI-FL	NBI-FR	NBI-DL	NBI-DR
Injection directions	co-current	co-current	counter-current	counter-current	co-current	co-current
$R_{\rm tan}$	1.26 m	0.73 m	0.61 m	1.14 m	1.14 m	0.61 m

The equilibrium of EAST (shot-77759) has been used in our simulation (the plasma current $I_{\rm p}=500\,{\rm kA}$, safety factor $q_{95}=5.33$, toroidal magnetic field $B_{\rm T}=-2.47\,{\rm T}$, electron temperature $T_{\rm e}=1.5\,{\rm keV}$, ion temperature $T_{\rm i}=0.8\,{\rm keV}$ and gapout is 0.045 m). During the simulation, the equilibrium, the background plasma parameters given above, and their profiles are unchanged. In addition, the effect of the background plasma rotation on the power deposition is not taken into account in our simulation. To get more accurate plasma density for the simulation, the following fitting formula is adopted:

$$n_{\rm e}(\rho)=n_{\rm e}(a)+[n_{\rm e}(0)-n_{\rm e}(a)][(1-\rho^b)^c+(1-\rho^2)^d]/2, \quad (1)$$

where ρ is the square root of the normalized toroidal magnetic flux, $n_{\rm e}(0)$ and $n_{\rm e}(a)$ represent the corresponding values of $n_{\rm e}(\rho)$ in the center and at the edge of the plasma. Furthermore, b, c and d are the profile's parameters. By comparing with the experimental data from POINT[18,19] as shown in Fig. 2 for the averaged electron density $\langle n_{\rm e}\rangle=3.1\times10^{19}\,{\rm m}^{-3}$, we choose the fitting parameters $(b,c,d)=(1.15,0.53,0.28)$. According to these settings, the average plasma density obtained from Eq. (1) is $3.1035\times10^{19}\,{\rm m}^{-3}$, which is consistent with the experiment data within the experimental error.

For NBI-AL and NBI-AR, by comparing the temperature variation of thermocouples embedded in the beam target tiles, we obtained the experimental data of the ST loss ratio for different densities ($\langle n_{\rm e}\rangle: 2.0\sim 3.6\times10^{19}\,{\rm m}^{-3}$, $E_{\rm nbi}=50\,{\rm keV}$) and different beam energies ($E_{\rm nbi}: 47\sim63\,{\rm keV}$, $\langle n_{\rm e}\rangle=3.0\times10^{19}\,{\rm m}^{-3}$) on EAST. Using Eq. (1) and the modules (NUBEAM, ONETWO and TRANSP), we have achieved the simulation ST loss ratio displayed in Fig. 3. During the simulation, full, half, and one-third energy fractions of the beam are kept constant; that is, $E:E/2:E/3=80\%:14\%:6\%$.

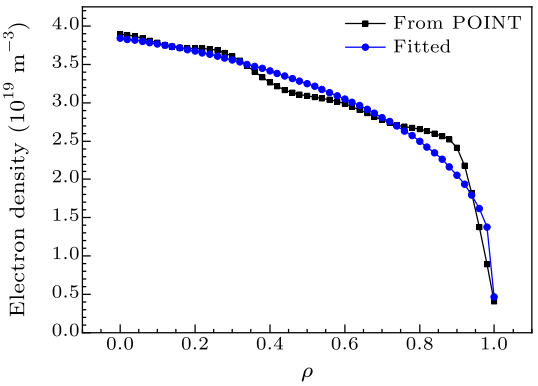

Fig. 2. Profiles of the electron density from POINT and the fitting formula (1).

Figure 3 shows that the simulation ST loss ratio is the basic rationality with the most experimental data within the experimental error. In addition, the simulation results illustrate that the ST loss ratio is an exponential function of plasma density and a linear function of beam energy, which are consistent with the conclusions on DIII-D[9] and ITER.[7]

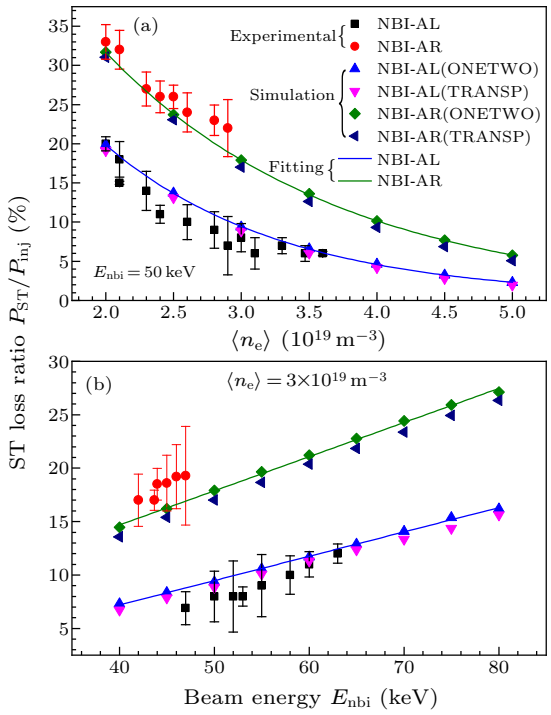

Fig. 3. Comparisons between the simulation and experimental data for the ST loss ratio (a) versus the density with $E_{\rm nbi} = 50\,{\rm keV}$, (b) versus $E_{\rm nbi}$ with $\langle n_{\rm e}\rangle = 3\times10^{19}\,{\rm m}^{-3}$.

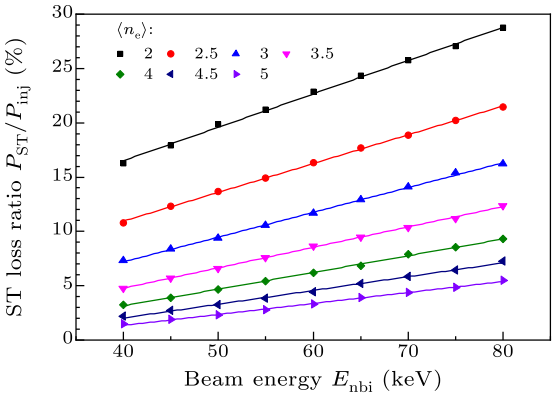

Fig. 4. ST loss ratio of NBI-AL versus beam energy for different plasma densities on EAST.

Furthermore, according to the theory of the beam power deposition and the experimental analysis given above, there are two major factors that affect the ST loss. Using NUBEAM/ONETWO, we have achieved the ST loss ratio for plasma density ($2.0 \sim 5.0\times10^{19}\,{\rm m}^{-3}$) and beam energy (40–80 keV). First, based on the linear relationship of ST loss ratio with beam energy, we obtained the linear fitting line when $\langle n_{\rm e}\rangle = 2.0\times10^{19}\,{\rm m}^{-3}$. The density was increased from 2.5 to $5.0\times10^{19}\,{\rm m}^{-3}$, and Fig. 4 illustrates different fitting lines whose slopes and intercepts vary with plasma density. Figures 5(a) and 5(b) display the slopes and intercepts of different fitting lines, respectively. Second, by applying the second fitting method on slopes and intercepts, we obtained a linear function of the slope and an exponential function of the intercept with the density. In the end, combining the multi-step fitting method given above, we achieved an analytical formula of ST loss ratio as the function of beam energy and plasma density for NBI-AL.

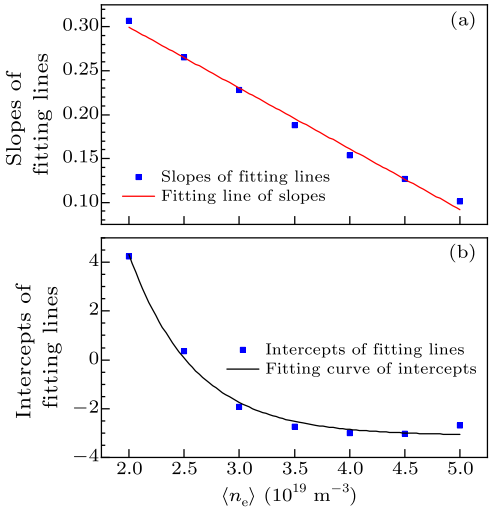

Fig. 5. (a) Slopes and (b) intercepts of different linear fitting lines for the ST loss ratio of NBI-AL.

Using the above multi-step fitting method on the simulation data for NBI-AR, NBI-FL, NBI-FR, NBI-DL and NBI-DR in Fig. 1, the ST loss ratio f in different beam paths on EAST are displayed in the following formulae:

$$\begin{aligned}
f_{\rm NBI-AL} &= (0.44 - 0.07\langle n_{\rm e}\rangle)E_{\rm nbi} \\
&\quad + 219.71\exp(-\langle n_{\rm e}\rangle/0.590) - 3.10, \\
f_{\rm NBI-AR} &= (0.49 - 0.06\langle n_{\rm e}\rangle)E_{\rm nbi} \\
&\quad + 143.60\exp(-\langle n_{\rm e}\rangle/0.967) - 4.63, \\
f_{\rm NBI-FL} &= (0.55 - 0.07\langle n_{\rm e}\rangle)E_{\rm nbi} \\
&\quad + 138.89\exp(-\langle n_{\rm e}\rangle/0.951) - 4.29, \\
f_{\rm NBI-FR} &= (0.55 - 0.09\langle n_{\rm e}\rangle)E_{\rm nbi} \\
&\quad + 299.40\exp(-\langle n_{\rm e}\rangle/0.578) - 3.11, \\
f_{\rm NBI-DL} &= (0.49 - 0.07\langle n_{\rm e}\rangle)E_{\rm nbi} \\
&\quad + 200.40\exp(-\langle n_{\rm e}\rangle/0.700) - 3.83, \\
f_{\rm NBI-DR} &= (0.49 - 0.06\langle n_{\rm e}\rangle)E_{\rm nbi} \\
&\quad + 134.30\exp(-\langle n_{\rm e}\rangle/1.027) - 4.71,
\end{aligned} \tag{2}$$

in units of 100%, $10^{19}\,{\rm m}^{-3}$, keV. According to the fitting formula given above, comparisons between the simulation and fitting data for NBI-AL and NBI-AR are shown in Fig. 6, which illustrates the accuracy of the fitting formulae (2). This figure also illustrates that the NBI-AR has a larger ST loss ratio due to the tangential radius smaller than NBI-AL.

In the end, we use NUBEAM/ONETWO modules to achieve the total beam heating percentage without MHD instabilities on EAST.

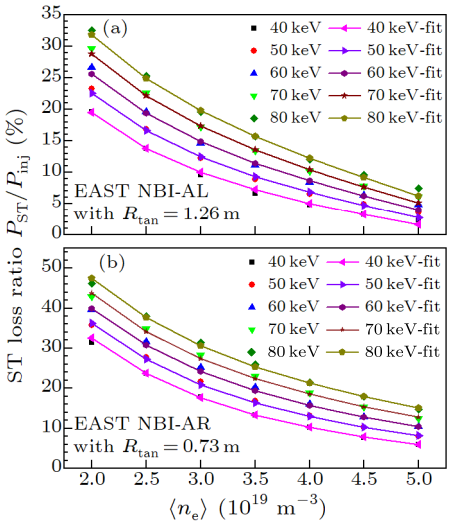

Fig. 6. Comparisons between the simulation values and the fitting data from Eq. (2) for (a) NBI-AL with $R_{\rm tan} = 1.26$ m (b) NBI-AR with $R_{\rm tan} = 0.73$ m.

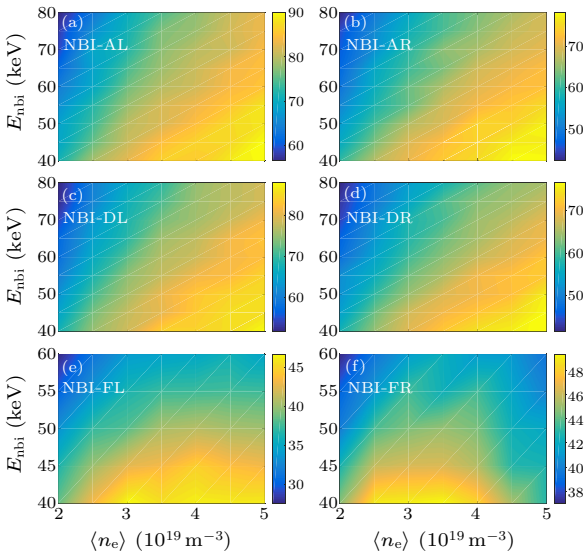

Fig. 7. Total heating percentages of different beams in Fig. 1 for plasma density and beam energy on EAST.

From Fig. 7, we can see that the total beam heating percentage increases with plasma density and decreases with beam energy for co-current NBI-A and NBI-D. The improvement of beam energy and the reduction of beam density result in the deeper penetration depth of the beam, which decreases the beam's heating efficiency. In addition, according to Fig. 7 and Table 1, we find that the beam heating percentage increases with the enlargement of tangential radius. This conclusion is consistent with the previous simulation conclusion on EAST.[5] Moreover, Fig. 7 shows that co-current NBI-D has a higher heating percentage than counter-current NBI-F, due to the different radial drift. Since co-current beam ions move inward and counter-current ones move outward, NBI-F has larger prompt loss and lower heating efficiency than NBI-D.

Table 2. The injected beam power $P_{\rm inj}$ (MW) versus beam energy $E_{\rm nbi}$ (keV) during EAST NBI physical experiments.

$E_{\rm nbi}$	40	45	50	55	60	65	70	75	80
$P_{\rm inj}$	0.5	0.67	0.82	1.0	1.19	1.38	1.568	1.77	1.96

During the EAST NBI physical experiments, the relationship between beam energy and injected beam power is shown in Table 2 based on the experimental beam data. Figure 8 illustrates the variation of the beam heating percentage of NBI-AL with the injected beam power and plasma density. From Fig. 8, we can find that the total beam heating percentage increases almost linearly with beam power and rises exponentially with plasma density. For NBI-A and NBI-D, Fig. 7 displays the similar relationships of heating percentages with beam energy and plasma density.

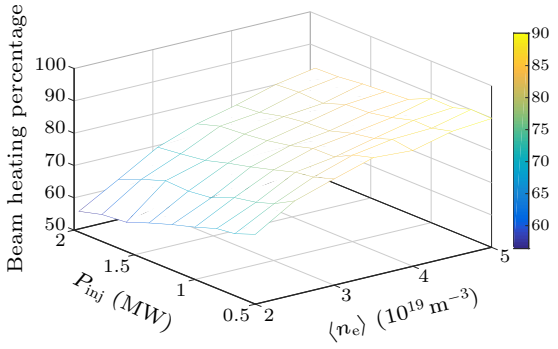

Fig. 8. Total beam heating percentage of NBI-AL versus plasma density and injected beam power on EAST.

Thus, according to the characteristics of beam heating percentage given above, the similar multi-step fitting method was also applied on NBI-AL, NBI-AR, NBI-DL and NBI-DR. The beam heating percentages H in different beam paths are expressed as follows:

$$\begin{aligned} H_{\rm NBI-AL} =& (1.84\langle n_e\rangle - 14.11)P_{\rm inj} \\ & -95.27\exp(-0.86\langle n_e\rangle) + 93.58, \\ H_{NBI-AR} =& (1.52\langle n_e\rangle - 14.41)P_{\rm inj} \\ & -109.6\exp(-0.87\langle n_e\rangle) + 83.29, \\ H_{\rm NBI-DL} =& (1.04\langle n_e\rangle - 13.01)P_{\rm inj} \\ & -100.93\exp(-0.78\langle n_e\rangle) + 82.53, \\ H_{NBI-DR} =& (1.76\langle n_e\rangle - 14.66)P_{\rm inj} \\ & -127.76\exp(-0.95\langle n_e\rangle) + 91.20, \end{aligned} \tag{3}$$

in units of 100%, 10^{19} m^{-3}, MW. These analytical expressions of the total beam heating percentage will be used in the preliminary evaluation of the beam heating and plasma performance during the high parameter physics experiments on EAST without MHD instabilities.

In summary, using NUBEAM, ONETWO and TRANSP modules and experimental data, we have verified the basic consistency between the simulation and experimental results within the experimental error. The analytical quantitative expressions of the ST

loss ratio as a function of beam energy and plasma density on EAST are achieved by applying the multi-step numerical fitting method. In addition, using the same method, we have obtained the analytical expressions of the total beam heating percentage with injected beam power and plasma density. These quantitative evaluations of the ST loss ratio and beam heating percentage will be applied to protect the safety and the high parameter experiments with NBI on EAST. Furthermore, this multi-step fitting method will also be applied to the numerical analysis of physical functions that are affected by many variables.

In addition to the two major factors given above (i.e., plasma density and beam energy), there are other factors that may affect the ST loss, such as electron temperature, plasma configuration, and energy fractions (at full, half, and one third energies). Other loss channels may also exist during the neutral beam power deposition, such as prompt loss, ripple loss and fast ion loss caused by MHD instabilities. Thus, to get a more accurate evaluation of the NBI heating, it is necessary to carry out a numerical simulation, as well as experimental studies about these loss channels in the future work.

Numerical computations were performed on the ShenMa High Performance Computing Cluster in Institute of Plasma Physics, Chinese Academy of Sciences. Part of this research used the computing resources from the Supercomputing Center of University of Science and Technology of China.

References

[1] Yu L M *et al.* 2019 *Nucl. Fusion* **59** 086016
[2] Chen W *et al.* 2017 *Nucl. Fusion* **57** 114003
[3] Yu D L *et al.* 2016 *Nucl. Fusion* **56** 056003
[4] Wang X Y *et al.* 2020 *Plasma Sci. Technol.* **22** 065104
[5] Wang J F *et al.* 2010 *Plasma Sci. Technol.* **12** 289
[6] Wu X Q *et al.* 2013 *Plasma Sci. Technol.* **15** 480
[7] Kadomtsev B B *et al.* 1990 *Nucl. Fusion* **30** 1675
[8] Wu B *et al.* 2011 *Fusion Eng.* **86** 947
[9] Riggs S, Hong R and Kessler D 1995 *Neutral Beam Shine-Through Power and Its Dependence on the Line Density of the DIII-D Plasma* in *16th IEEE/NPSS Symposium on Fusion Engineering*, Champaign, Illinois, vols 1 & 2 p 856
[10] Polevoi A R *et al.* 2013 *Nucl. Fusion* **53** 123026
[11] Snicker1 A *et al.* 2017 *Neutral Beam Ion Shine-through Calculations for Reduced Field Current Plasmas ITER* in *45th EPS Conference on Plasma Physics* p 1.1067
[12] Pankin A *et al.* 2004 *Comput. Phys. Commun.* **164** 421
[13] Attenberger S E *et al.* 1987 *J. Comput. Phys.* **72** 435
[14] Mandrekas J 1992 *Physics Models and User's Guide for the Neutral Beam Module of the SuperCode*, Georgia Institute of Technology, Atlanta, USA, Tech. Rep. GTFR-102
[15] ONETWO: Https://Fusion.Gat.Com/Theory/Onetwo/
[16] Hawryluk R J 1981 *Physics of Plasmas Close to Thermonuclear Conditions* , in *Proceedings of the Course Held in Varenna* Italy, 27 August–8 September 1979, pp 19–46
[17] Wu B *et al.* 2017 *Plasma Phys. Control. Fusion* **59** 025004
[18] Liu H Q *et al.* 2016 *Rev. Sci. Instrum.* **87** 11D903
[19] Qian J P *et al.* 2017 *Nucl. Fusion* **57** 036008